Hindawi Publishing Corporation
International Journal of Photoenergy
Volume 2012, Article ID 618642, 9 pages
doi:10.1155/2012/618642

Research Article

Effect of Al-Cu Bimetallic Components in a TiO_2 Framework for High Hydrogen Production on Methanol/Water Photo-Splitting

A-Young Kim and Misook Kang

Department of Chemistry, College of Science, Yeungnam University, Gyeongbuk, Gyeongsan 712-749, Republic of Korea

Correspondence should be addressed to Misook Kang, mskang@ynu.ac.kr

Received 29 August 2011; Revised 3 January 2012; Accepted 3 January 2012

Academic Editor: Gongxuan Lu

This study investigated the production of hydrogen over TiO_2, Cu-TiO_2, Ag-TiO_2, and Cu-Ag-TiO_2 photocatalysts incorporated with Cu and Ag ions by a solvothermal method. The Ag metal (200, 220, and 311 plane) peaks at $2\theta = 44.50, 64.00$, and 77.60^{o} were presented in the Ag-incorporated TiO_2 catalysts. The CuO component ($Cu2p_{3/2}$ and $Cu2p_{1/2}$ at 930.4 and 949.5 eV) was exhibited in the X-ray photon spectroscopy (XPS) band of the Cu-incorporated TiO_2 photocatalyst. All the absorption plots in the Cu-, Ag-, and Cu-Ag-incorporated catalysts showed excitation characteristics; an asymmetric tail was observed towards a higher wavelength due to scattering. The intensity of the photoluminescence (PL) curves of Cu-Ag-TiO_2s was smaller, with the smallest case being observed for Cu(0.05)-Ag(0.05)Ti(0.9)O_2 and Cu(0.03)-Ag(0.07)Ti(0.9)O_2. Based on these optical characteristics, the production of H_2 from methanol/water photodecomposition over the Cu(0.03)-Ag(0.07)Ti(0.9)O_2 photocatalyst at 8,750 mmol after 8 h was greater than that over the other photocatalysts.

1. Introduction

The technology for generating hydrogen by the splitting of water using a photocatalyst has attracted much attention. The principle of photocatalytic water decomposition is based on the conversion of light energy into electricity in a semiconductor on exposure to light [1–3]. Semiconductor materials such as $MTiO_3$ [4, 5] and TiO_xN_y [6, 7] have been widely investigated due to their low band gap and high corrosion resistance. However, the photocatalytic decomposition of water on a TiO_2 photocatalyst is ineffective as the amount of hydrogen produced is limited by the rapid recombination of holes and electrons, resulting in the formation of water. Recently, the production of hydrogen has been extended to the photodecomposition of methanol (CH_3OH), which has a lower splitting energy than water. The following overall methanol decomposition reaction was proposed [8, 9]:

$$\mathrm{MeOH(l)} \leftrightarrow \mathrm{HCHO(g)} + \mathrm{H_2(g)}, \mathrm{G_1}^{\circ} = 64.1\,\mathrm{kJ\,mol^{-1}}, \quad (1)$$

$$\mathrm{HCHO(g)H_2O(l)} \leftrightarrow \mathrm{HCO_2H(l)} + \mathrm{H_2(g)}, \quad \mathrm{G_2^{\circ}} = 47.8\,\mathrm{kJ\,mol^{-1}}, \quad (2)$$

$$\mathrm{HCO_2H\ (l)} \longleftrightarrow \mathrm{CO_2(g)} + \mathrm{H_2(g)}, \mathrm{G_3}^{\circ} = -95.8\,\mathrm{kJ\,mol^{-1}}. \quad (3)$$

$$\text{Finally,}\ \ \mathrm{MeOH(l)} + \mathrm{H_2O\ (l)} \leftrightarrow \mathrm{CO_2(g)} + 3\mathrm{H_2(g)}, \quad \Delta\mathrm{G}^{\circ} = 16.1\,\mathrm{KJ\,mol^{-1}}. \quad (4)$$

The decomposition energy for methanol is smaller than 0.7 eV, compared to 1.2 eV for water splitting. Most investigations on the production of hydrogen via methanol photodecomposition have focused on M_xO_y (M = Cd or Zn) [10, 11] and noble metal (Cu, Ag, Pd, Pt, Au)-doped TiO_2 [12–16], which can be used to activate the photocatalysts using UV light with longer wavelengths. However, the number of known photocatalysts is limited, and their activities remain low. New photocatalysts possessing greater hydrogen-producing activity under visible light irradiation

need to be developed. Moreover, hydrogen-based energy offers the significant advantage of being environmentally friendly. In our previous study [17], a new material, Cu-TiO_2, where Cu_xO was substituted into the TiO_2 framework, was investigated as a conducting component to reduce the large band gap of pure TiO_2. The structural effect of the catalyst on photocatalysis was also evaluated using Cu-incorporated TiO_2 photocatalysts with anatase and rutile structures. The production reached 16,000 μmol after 24 h over Cu-TiO_2 with a rutile structure for water/methanol decomposition. Additionally, in our other paper [18], we reported about the synthesis and characterization of Ag_xO and found that the hydrogen production from methanol photodecomposition over a mixture of Ag_xO and TiO_2 was remarkably increased. Moreover, it was further enhanced when Ag_xO thermally treated at 100°C was added, and the production peaked at 17,000 μmol after 24 h. However, the economic evaluation of this hydrogen production process remained poor, and any Ag and Cu metals remaining after the reaction showed a tendency to precipitate at the bottom of the reactor, where they were rapidly reduced. Subsequently the catalyst was rapidly deactivated.

Therefore, in order to overcome these disadvantages, we prepared a new catalyst in which two metals with different reduction/oxidation abilities were embedded into the TiO_2 framework. We investigated the production of hydrogen from the methanol/water photodecomposition over TiO_2, Cu(0.1)-Ti(0.9)O_2, Ag(0.1)-Ti(0.9)O_2, Cu(0.05)-Ag(0.05) Ti(0.9)O_2, Cu(0.03)-Ag(0.07)Ti(0.9)O_2, and Cu(0.07)-Ag(0.03)Ti(0.9)O_2 photocatalysts in which Cu and Ag ions were incorporated into the TiO_2 framework with an anatase structure, prepared using a solvothermal method. To determine the relationship between Cu and Ag species and the catalytic performance for the production of H_2, these photocatalysts were examined using X-ray diffraction analysis (XRD), X-ray photon spectroscopy (XPS), and UV-visible and photoluminescence (PL) spectroscopy.

2. Experimental

2.1. Preparation of Photocatalysts. The photocatalysts were prepared using the conventional solvothermal method, as shown in Figure 1. To prepare the sol mixture, titanium tetraisopropoxide (TTIP, 99.95%), copper nitrate ($Cu(NO_3)_2$, 99.9%), and silver nitrate ($AgNO_3$, 99.9%), all supplied by Junsei Chemical (Tokyo, Japan), were used as the titanium, copper, and silver precursors, respectively. After 0.9 mol TTIP was added slowly to 250 mL ethanol, Ag and Cu nitrate (totally 10 mol-% per titanium mole) dissolved with ethanol were added into the titanium solution. The mixture was stirred homogeneously for 1 h, and the pH was maintained at 3.0. The final solution was stirred homogeneously and moved to an autoclave for the thermal treatment. TTIP, silver, and copper nitrates were hydrolyzed *via* the OH groups during thermal treatment at 473 K for 8 h under a nitrogen environment at a pressure of approximately 10 atm. The resulting precipitate was washed with distilled water until pH = 7.0 and then dried at 353 K for 24 h. The six photocatalysts were pure TiO_2, Cu(0.1)-Ti(0.9)O_2, Ag(0.1)-Ti(0.9)O_2, Cu(0.05)-Ag(0.05)Ti(0.9)O_2, Cu(0.03)-Ag(0.07)Ti(0.9)O_2, and Cu(0.07)-Ag(0.03)Ti(0.9)O_2.

2.2. Characteristics of the Photocatalysts. The powders for the six synthesized photocatalysts were examined by XRD (MPD, PANalytical, at Yeungnam University Instrumental Analysis Center) with nickel-filtered CuKα radiation (30 kV, 30 mA) at 2θ angles ranging from 10 to 80°, a scan speed of 10° min^{-1}, and a time constant of 1 s. The sizes and shapes of the particles were measured by transmission electron spectroscopy (TEM; H-7600, Hitachi, at Yeungnam University Instrumental Analysis Center) operated at 120 kV. The UV-visible spectra were obtained using a Cary 500 spectrometer with a reflectance sphere over the special range of 200 to 800 nm. PL spectroscopy was also performed to determine the number of photo-excited electron hole pairs using a PL mapping system (LabRamHR, Jobin Yvon, at Korea Photonics Technology Institute Material Characterization Center). It was also used to examine the number of photo-excited, electron-hole pairs for all samples. Samples of 1.0-mm diameter pellets were measured at room temperature using a He-Cd laser source at 325 nm in the reflection mode. XPS measurements of Cu2p, Ag3d, Ti2p, and O1s were recorded with an ESCA 2000 (VZ MicroTech, Oxford, UK) system, equipped with a nonmonochromatic AlK (1486.6 eV) X-ray source. The powders were pelletized at 1.2×10^4 kPa for 1 min, and the 1.0-mm pellets were then maintained overnight in a vacuum (1.0×10^{-7} Pa) to remove the water molecules from the surface prior to the measurement. The base pressure of the ESCA system was below 1×10^{-9} Pa. Experiments were recorded with a 200-W source power and an angular acceptance of ±5°. The analyzer axis made an angle of 90° with the specimen surface. Wide scan spectra were measured over a binding energy range of 0 to 1200 eV, with pass energy of 100.0 eV. The Ar^+ bombardment of the photocatalysts was performed with an ion current of 70 to 100 nA, over an area of 10.0×10.0 mm, with a total sputter time of 2400 s divided into 60 s intervals. A Shirley function was used to subtract the background in the XPS data analysis. The O1s, Ti2p, Ag3d, and Cu2p XPS signals were fitted using mixed Lorentzian-Gaussian curves.

2.3. H_2 Production from Methanol/Water Photo Decomposition over Photocatalysts. The photodecomposition of methanol/water was performed using a liquid photoreactor designed in our laboratory (Figure 2). For methanol/water photodecomposition, 0.5 g of the powdered photocatalysts was added to 2.0 L of a 1.0 : 1.0 methanol/water mixture in a 3.0-L Pyrex reactor. UV-lamps (6×3 Wcm^{-2} = 18 Wcm^{-2}, 30 cm length × 2.0 cm diameter; Shinan, Sunchun, Korea), emitting radiation at 365 nm, were used. The methanol/water decomposition was conducted for 30 h, with stirring, with the hydrogen evolution determined after 1 h. The hydrogen (H_2) produced during the methanol/water photodecomposition was analyzed using a thermal-conductivity-detector-(TCD-) type gas chromatograph (GC, model DS 6200;

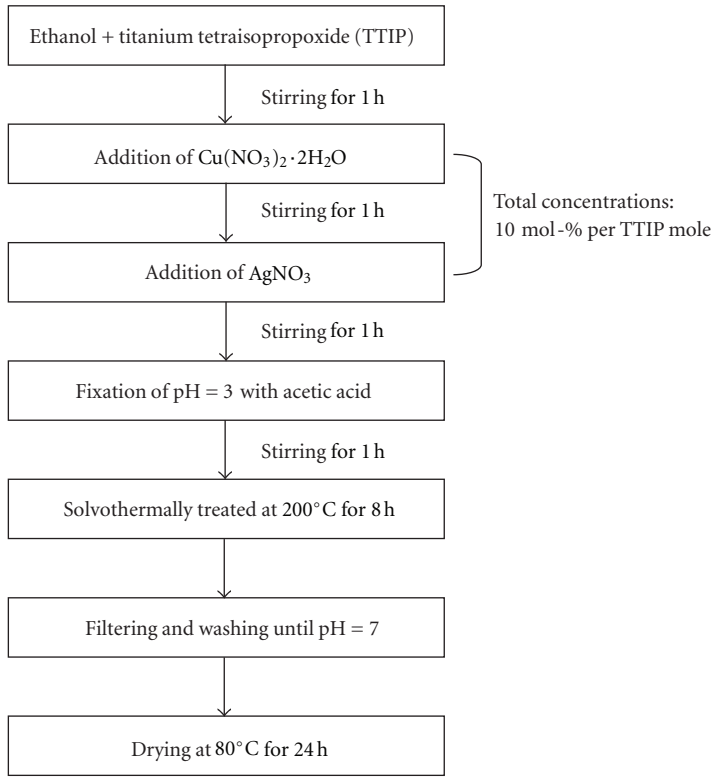

Figure 1: The preparation of six photocatalysts, pure TiO_2, Cu(0.1)-Ti(0.9)O_2, Ag(0.1)-Ti(0.9)O_2, Cu(0.05)-Ag(0.05)Ti(0.9)O_2, Cu(0.03)-Ag(0.07)Ti(0.9)O_2, and Cu(0.07)-Ag(0.03)Ti(0.9)O_2 using a solvothermal method.

Donam Instruments Inc., Gyeonngi-do, Korea). To determine the products and intermediates, the GC was directly connected to the methanol/water decomposition reactor. The GC conditions were as follows: column: Carbosphere (Alltech, Deerfield, IL, USA), injection temp.: 160°C, initial temp.: 100°C, final temp.: 100°C, and detector temp.: 200°C.

3. Results and Discussion

3.1. Characteristics of the Photocatalysts. Figure 3 shows the XRD patterns for the six as-synthesized photocatalysts. Generally, TiO_2 and metal-TiO_2 photocatalysts with an anatase structure are known to perform well in the decomposition of various organic compounds. The diffraction peaks for the anatase and rutile phases are labeled A and R with the corresponding diffraction planes given in parentheses, respectively [19]. Both pure TiO_2 and metal-incorporated TiO_2 catalysts showed well-developed anatase structures as synthesized. The Ag metal (200, 220, and 311 plane) peaks at $2\theta = 44.50$, 64.00, and 77.60° were presented in the Ag-incorporated TiO_2 catalysts [20] and the intensities increased with increasing amount of loaded Ag. These results indicated that the Ag components partially existed on the external surface of TiO_2 and were unlikely to be incorporated into the framework of the anatase structure. However, the Cu component did not appear in any of the catalysts, which indicated its complete insertion into the TiO_2 framework. Interestingly, the structural stability of anatase increased when bimetallic two metals, Cu and Ag, were inserted into the TiO_2 framework at the same time, compared with when one kind of metal, Cu or Ag, that was inserted. Generally, crystalline domain sizes decrease with increasing line broadening of the peaks. The line broadening of the [101] peak is related to the size of the hexagonal crystalline phase. Scherrer's equation [21], $t = 0.9\lambda/\beta \cos\theta$, where λ is the wavelength of the incident X-rays, β is the full width at half maximum height (FWHM) in radians, and θ is the diffraction angle, was used to estimate the crystalline domain size. The estimated crystalline domain sizes were 15.04, 13.71, 17.00, 11.80, 15.82, and 15.25 nm for pure TiO_2, Cu(0.1)-Ti(0.9)O_2, Ag(0.1)-Ti(0.9)O_2,Cu(0.05)-Ag(0.05)Ti(0.9)O_2, Cu(0.03)-Ag(0.07)Ti(0.9)O_2, and Cu(0.07)-Ag(0.03)Ti(0.9)O_2 powders, respectively. The results indicated that the grain growths increased and decreased according to incorporation of Ag and Cu, respectively.

Figure 4 shows TEM images of the particle shapes of the six photocatalysts. A relatively uniform mixture of rhombic and cubic particles was observed with sizes ranging from 10 to 20 nm. The particles were slightly decreased in size when Cu was added but enlarged with Ag addition. The size was the smallest in Cu(0.05)-Ag(0.05)Ti(0.9)O_2, which corresponds to the XRD patterns shown in Figure 3.

Table 1 summarizes the atomic composition of the six photocatalysts. The compositions were estimated using energy dispersive X-ray (EDAX) analysis. The ratios of metal

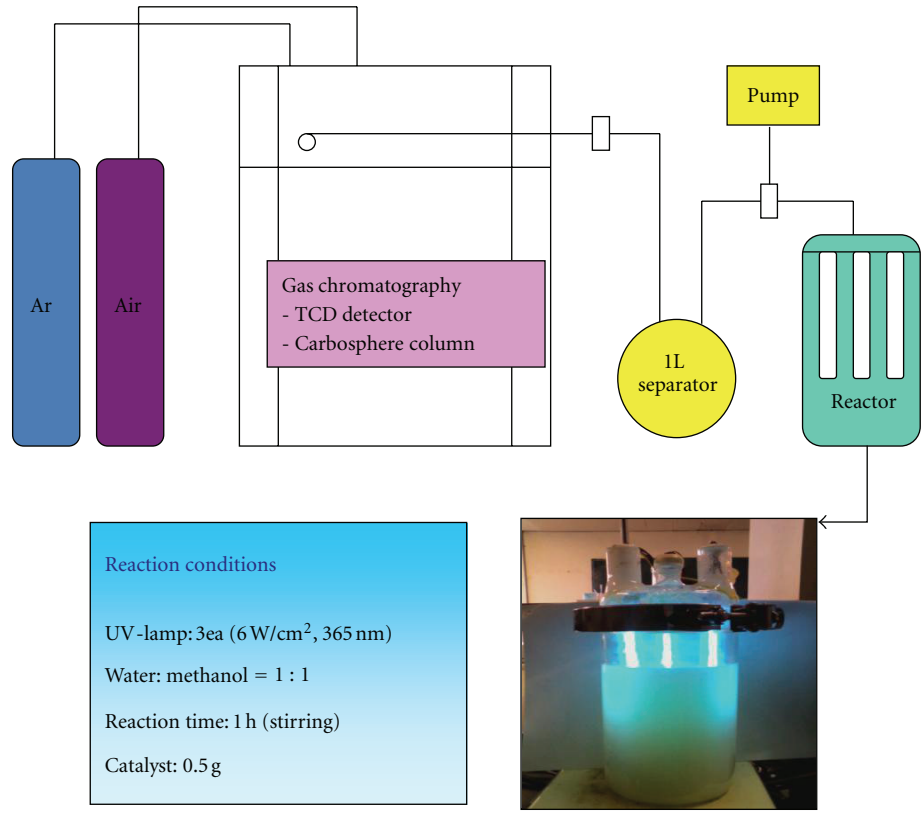

Figure 2: The liquid photoreactor used for H_2 production via methanol/water photodecomposition. Reaction conditions: volumetric ratio of CH_3OH/H_2O = 1; catalyst weight per 2.0 L solution, 0.5 g; UV intensity at 365 nm, 18 W m^{-2}; batch system.

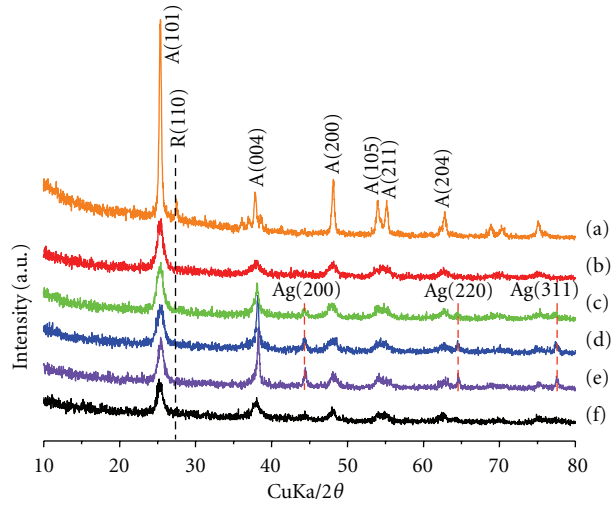

Figure 3: The XRD patterns of six photocatalysts as-synthesized. (a) TiO_2, (b) Cu(0.1)-Ti(0.9)O_2, (c) Cu(0.07)-Ag(0.03)Ti(0.9)O_2, (d) Cu(0.05)-Ag(0.05)Ti(0.9)O_2, (e) Cu(0.03)-Ag(0.07)Ti(0.9)O_2, and (f) Ag(0.1)-Ti(0.9)O_2.

(mono or bimetal)/Ti were 0.20, 0.10, 0.16, 0.10, and 0.11 in Cu(0.1)-Ti(0.9)O_2, Ag(0.1)-Ti(0.9)O_2, Cu(0.05)-Ag(0.05)Ti(0.9)O_2, Cu(0.03)-Ag(0.07)Ti(0.9)O_2, and Cu(0.07)-Ag(0.03)Ti(0.9)O_2 powders, respectively. Similar to the XRD results, the incorporation of Ag component into the TiO_2 framework was more difficult than that of Cu component.

Figure 5 shows the UV-visible spectra of the six photocatalysts. The absorption of the Ti^{4+} tetrahedral symmetry normally appears at around 350 nm [22], which is assigned to L-L ($P \rightarrow \pi$ or $P \rightarrow \pi^*$) transitions localized on the oxygen. In the figure, the absorption bands are around 350 nm for all the photocatalysts, but the intensity of absorption

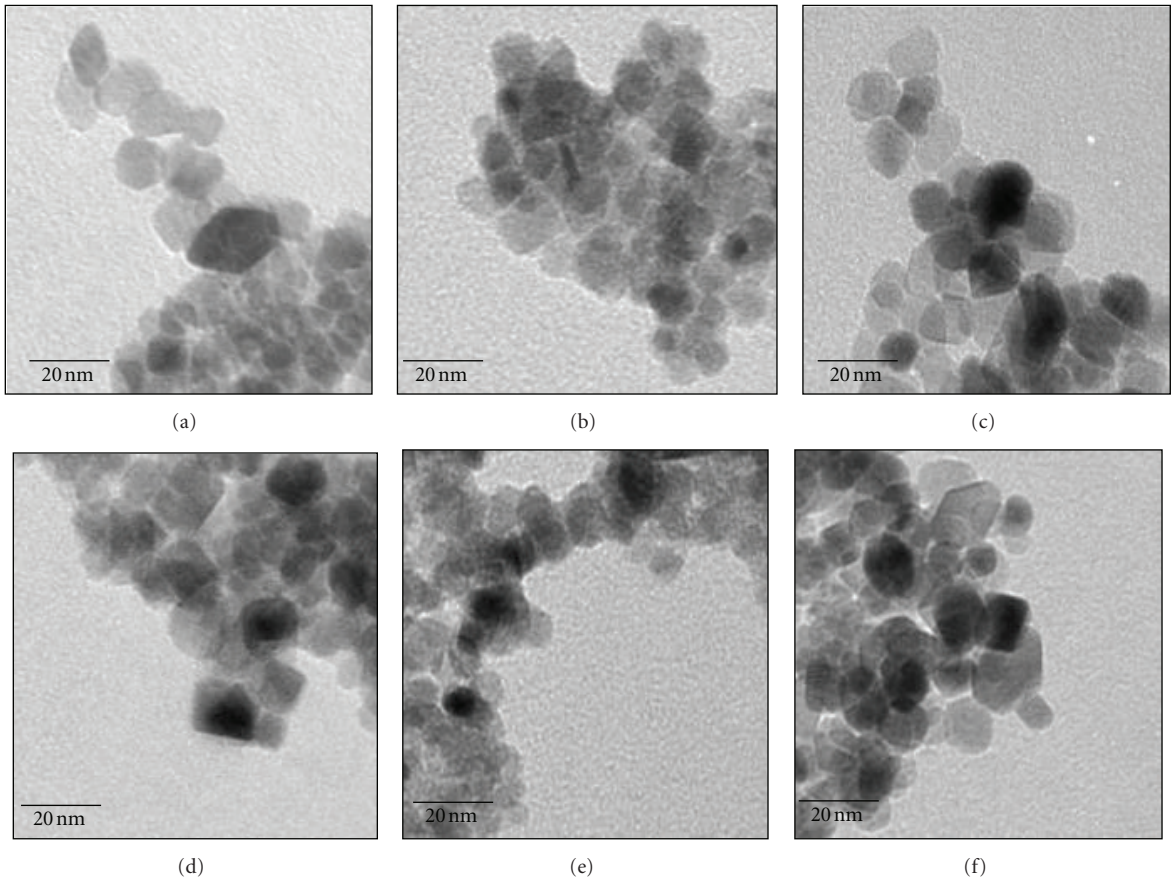

Figure 4: The TEM images of six photocatalysts as-synthesized.

Table 1: The atomic composition of the six photocatalysts.

	Atomic composition (%)				
Samples	Metal/Ti	O	Ti	Cu	Ag
TiO_2	—	7.167	28.33	—	—
Cu(0.1)-Ti(0.9)O_2	0.20	76.99	19.11	3.89	—
Ag(0.1)-Ti(0.9)O_2	0.10	74.03	23.56	—	2.41
Cu(0.05)-Ag(0.05)Ti(0.9)O_2	0.11	69.85	27.24	2.11	0.79
Cu(0.03)-Ag(0.07)Ti(0.9)O_2	0.16	70.78	25.25	2.03	1.94
Cu(0.07)-Ag(0.03)Ti(0.9)O_2	0.10	71.64	25.27	0.86	1.74

for pure TiO_2 is stronger than for metal-incorporated TiO_2. The Cu-incorporated materials broadly absorbed at around 650 nm with remarkable intensity, which is allowed by the large spin-orbit coupling constant of the d-d transfer of copper, and the band observed in the visible region can be rationalized in terms of symmetry arguments. Otherwise, the broad band in the Ag-incorporated catalysts at 380 ~ 600 nm was attributed to Ag → O metal-to-ligand charge transfer (MLCT) transitions. The two broad bands observed in the wavelength interval 350–600 nm were therefore assigned to the MLCT and d-d transitions, which indicated that the band gap was narrowed in the Ag- and Cu-inserted TiO_2 catalysts, leading to higher photocatalytic performance.

Figure 6 shows the PL spectra of the six photocatalysts. The PL curve suggests that the electrons in the valence band were transferred to the conduction band, after which the excited electrons were stabilized by photoemission. In general, it is very important that the PL intensity increases with the increasing number of emitted electrons resulting from the recombination between excited electrons and holes, and, consequently, that the photoactivity decreases [23]. In particular, the PL intensity decreases to a greater extent in the presence of a metal that can capture excited electrons or exhibit conductivity, via the relaxation process. The PL curve of pure TiO_2 showed emission at 370–450 nm as a curve type. The band broadening was attributed to the

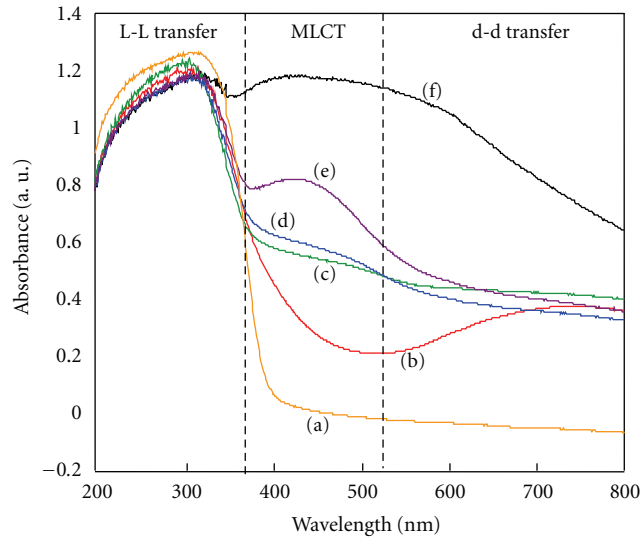

Figure 5: The UV-visible spectra of six photocatalysts as-synthesized. (a) TiO_2, b) Cu(0.1)-Ti(0.9)O_2, (c) Cu(0.07)-Ag(0.03)Ti(0.9)O_2, (d) Cu(0.05)-Ag(0.05)Ti(0.9)O_2, (e) Cu(0.03)-Ag(0.07)Ti(0.9)O_2, and (f) Ag(0.1)-Ti(0.9)O_2.

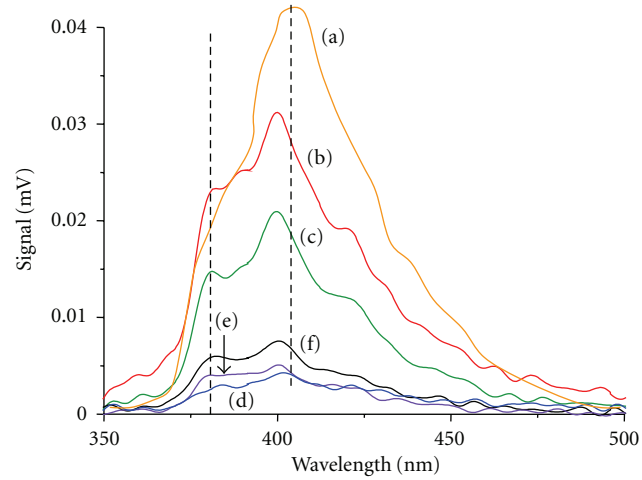

Figure 6: The PL spectra of six photocatalysts as-synthesized. (a) TiO_2, (b) Cu(0.1)-Ti(0.9)O_2, (c) Cu(0.07)-Ag(0.03)Ti(0.9)O_2, (d) Cu(0.05)-Ag(0.05)Ti(0.9)O_2, e) Cu(0.03)-Ag(0.07)Ti(0.9)O_2, and (f) Ag(0.1)-Ti(0.9)O_2.

overlapped emission from the higher and lower excited states to the ground states. The pattern of the Ag- or Cu-incorporated catalysts showed two curves—at 360 nm and 400 nm—which were attributed to the band gap between the incorporated metals, Ag or Cu, respectively, and that of pure anatase TiO_2. Additionally the curves were shifted to a lower wavelength, and the PL intensity decreased significantly with decreasing metal insertion, probably due to the electron-capturing actions of the metal atoms from conduction band of TiO_2. Particularly when Ag component was inserted into the TiO_2 framework, the PL intensity was largely reduced. Consequently, the PL intensity varied according to whether the added metal acted as an electron capturer or not. If the incorporated metals existed on the surface or in the framework of TiO_2, they attracted the excited electrons from TiO_2, so that the recombination of an electron and a hole was difficult, thus increasing the number of holes over the valence band and generating more OH radicals.

3.2. H_2 Production from Methanol/Water Decomposition over the Six Photocatalysts. Figure 7 summarizes the evolution of H_2 from methanol/water decomposition over the six photocatalysts in a batch-type, liquid photosystem. Over pure anatase TiO_2, 200 mmol of H_2 were only collected after methanol/water photodecomposition for 8 h, however the amount of H_2 gas more increased in the Ag- or Cu-incorporated photocatalysts linearly with increasing time. The H_2production was the highest in Cu(0.03)-Ag(0.07) Ti(0.9)O_2 at 8,750 mmol and finally reached 20,000 mmol after 30 h. therefore, the simultaneously bimetallic addition of Ag and Cu components had a greater influence on the H_2 production during methanol/water photodecomposition

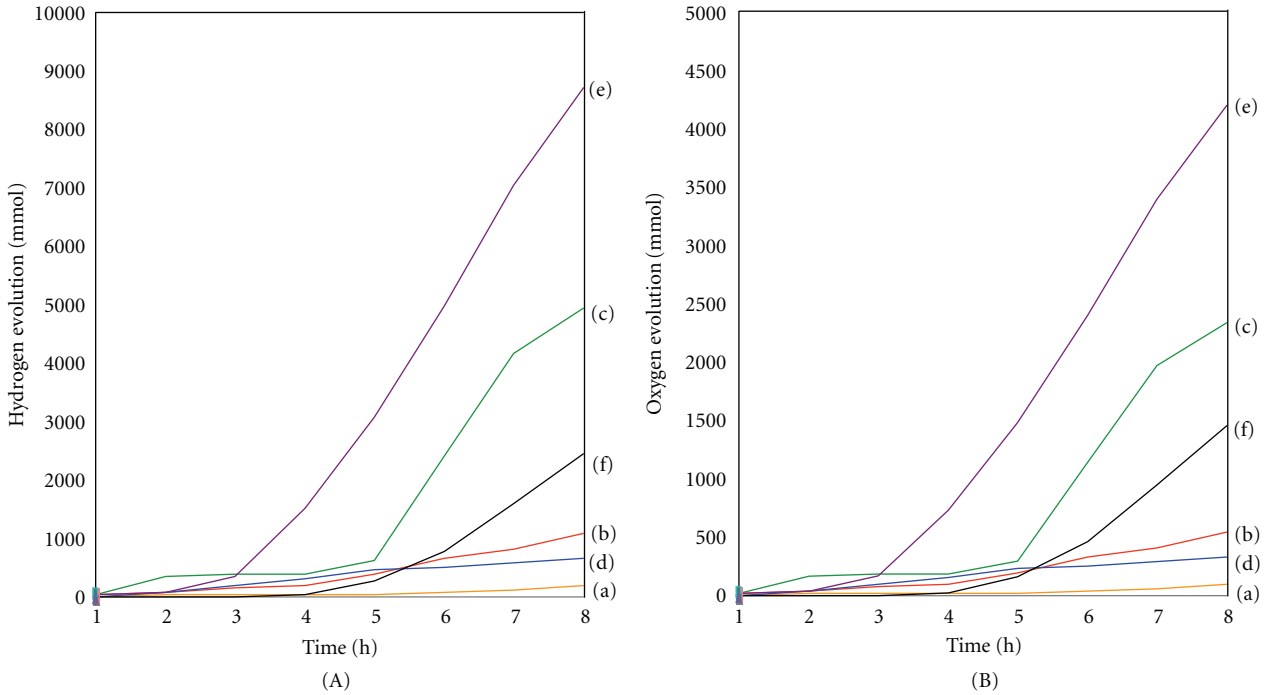

Figure 7: The evolution of H_2 from methanol/water decomposition over the six photocatalysts in a batch-type liquid photosystem. (A) accumulated amount of hydrogen gas and (B) accumulated amount of oxygen gas. (a) TiO_2, (b) Cu(0.1)-Ti(0.9)O_2, (c) Cu(0.07)-Ag(0.03)Ti(0.9)O_2, (d) Cu(0.05)-Ag(0.05)Ti(0.9)O_2, (e) Cu(0.03)-Ag(0.07)Ti(0.9)O_2, and f) Ag(0.1)-Ti(0.9)O_2.

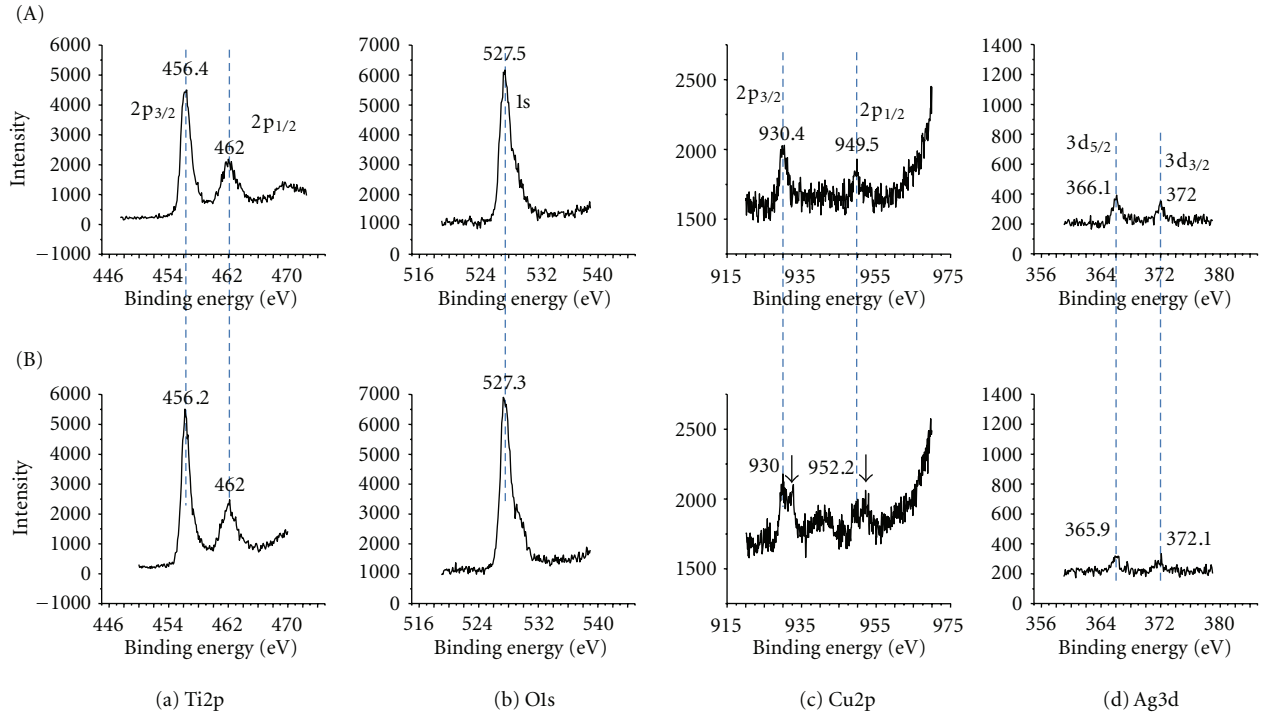

Figure 8: The XPS for Cu2p, Ag3d, Ti2p, and O1s of Cu(0.03)-Ag(0.07)Ti(0.9)O_2 before and after the methanol/water photodecomposition reaction: (A) before reaction and (B) after reaction.

than the mono metals, Cu- or Ag-incorporated TiO_2. Particularly, metal chunks were observed to be deposited in the reactor after the reaction. These results are evidence for the continuing oxidation/reduction actions between Cu and Ag during the reaction.

The Cu(0.03)-Ag(0.07)Ti(0.9)O_2 particles underwent quantitative XPS analyses before and after the reaction, with the typical survey and high-resolution spectra shown in Figure 8. The $Ti2p_{1/2}$ and $Ti2p_{3/2}$ spin-orbital splitting photoelectrons for anatase TiO_2s were located at binding energies of 462.0 and 456.4 eV, respectively, and were assigned to the presence of typical Ti^{4+} [24]. The measured FWHM of the $Ti2p_{3/2}$ peak was larger before reaction than after the reaction. However, there was no subsequent change. In general, a greater FWHM implies a greater amount of less-oxidized metals. The $Cu2p_{3/2}$ and $Cu2p_{1/2}$ spin-orbital splitting photoelectrons for the anatase Cu(0.03)-Ag(0.07)Ti(0.9)O_2 photocatalyst before the reaction were located at binding energies of 930.4 and 949.5 eV, respectively, and these bands were assigned to CuO. However, these bands were separated into two peaks at binding energies of 932.5 eV of $Cu2p_{3/2}$ and 952.5 eV of $Cu2p_{1/2}$, and these bands were assigned to Cu_2O [24]. On the other hand, the fresh photocatalyst showed $Ag3d_{5/2}$ and $Ag3d_{3/2}$ spin-orbital splitting photoelectrons at binding energies of 366.1 and 372.0 eV, respectively, which were assigned to AgO, but the peak intensities were dramatically decreased after the reaction. This result indicated that the oxidation state of Cu was reduced and the amount of AgO was decreased during the reaction, which enabled their strong involvement in methanol/water decomposition. The O1s region was decomposed into two contributions: metal (Ti^{4+} or Ti^{3+})-O (527.5 eV) in the metal oxide and metal-OH (529.5.0 eV). The ratios of metal-OH/metal-O in the O1s peaks were decreased after the reaction compared to that before the reaction. Additionally, the measured FWHM of the O1s peak was larger after reaction than that before, which was attributed to the exposure of Ag or Cu ions from the surface of TiO_2.

4. Conclusions

TiO_2 photocatalysts inserted with Ag, Cu, and Cu-Ag were prepared for the production of H_2 gas from methanol/water photodecomposition in a batch-type liquid photosystem. Compared to monometal-incorporated TiO_2, the H_2 production via methanol/water photodecomposition was markedly enhanced in bimetal-incorporated photocatalyst and reached 8,750 mmol after methanol/water photodecomposition for 8 h over Cu(0.03)-Ag(0.07)Ti(0.9)O_2 photocatalyst. These results confirmed that the simultaneous presence of Cu and Ag components in the framework of the TiO_2 anatase structure improved the H_2 production via methanol/water photodecomposition. Here, we suggested that any Cu or Ag components present in the TiO_2 framework are reduced or decreased by attracting the excited electrons from the valence band of TiO_2, because of the greater reduction potential of CuO or AgO than that of pure TiO_2. This hinders the recombination of an electron and a hole because the CuO or AgO component captures electrons, thereby increasing the number of holes over the valence band and allowing methanol decomposition to continue. The simultaneous insertion of the two ions into the TiO_2 framework induced an increased synergistic effect.

Acknowledgments

This research was supported by a Yeungnam University Research Grant, no. 210-A-380-115, and the authors are very grateful for this support.

References

[1] M. Ni, M. K. H. Leung, D. Y. C. Leung, and K. Sumathy, "A review and recent developments in photocatalytic water-splitting using TiO_2 for hydrogen production," *Renewable and Sustainable Energy Reviews*, vol. 11, no. 3, pp. 401–425, 2007.

[2] R. Dholam, N. Patel, M. Adami, and A. Miotello, "Hydrogen production by photocatalytic water-splitting using Cr- or Fe-doped TiO_2 composite thin films photocatalyst," *International Journal of Hydrogen Energy*, vol. 34, no. 13, pp. 5337–5346, 2009.

[3] L. S. Yoong, F. K. Chong, and B. K. Dutta, "Development of copper-doped TiO_2 photocatalyst for hydrogen production under visible light," *Energy*, vol. 34, no. 10, pp. 1652–1661, 2009.

[4] H. Mizoguchi, K. Ueda, M. Orita et al., "Decomposition of water by a $CaTiO_3$ photocatalyst under UV light irradiation," *Materials Research Bulletin*, vol. 37, no. 15, pp. 2401–2406, 2002.

[5] T. Ishii, H. Kato, and A. Kudo, "H_2 evolution from an aqueous methanol solution on $SrTiO_3$ photocatalysts codoped with chromium and tantalum ions under visible light irradiation," *Journal of Photochemistry and Photobiology A*, vol. 163, no. 1-2, pp. 181–186, 2004.

[6] T. Sreethawong, S. Laehsalee, and S. Chauadej, "Comparative investigation of mesoporous- and non-mesoporous-assembled TiO_2 nanocrystals for photocatalytic H_2 production over N-doped TiO_2 under visible light irradiation," *International Journal of Hydrogen Energy*, vol. 33, no. 21, pp. 5947–5957, 2008.

[7] J. Yuan, M. Chen, J. Shi, and W. Shangguan, "Preparations and photocatalytic hydrogen evolution of N-doped TiO_2 from urea and titanium tetrachloride," *International Journal of Hydrogen Energy*, vol. 31, no. 10, pp. 1326–1331, 2006.

[8] R. Gao, J. Stark, D. W. Bahnemann, and J. Rabani, "Quantum yields of hydroxyl radicals in illuminated TiO_2 nanocrystallite layers," *Journal of Photochemistry and Photobiology A*, vol. 148, no. 1–3, pp. 387–391, 2002.

[9] J. Chen, D. F. Ollis, W. H. Rulkens, and H. Bruning, "Photocatalyzed oxidation of alcohols and organochlorides in the presence of native TiO_2 and metallized TiO_2 suspensions—part (II): photocatalytic mechanisms," *Water Research*, vol. 33, no. 3, pp. 669–676, 1999.

[10] R. M. Navarro, F. del Valle, and J. L. G. Fierro, "Photocatalytic hydrogen evolution from CdS–ZnO–CdO systems under visible light irradiation: effect of thermal treatment and presence of Pt and Ru cocatalysts," *International Journal of Hydrogen Energy*, vol. 33, no. 16, pp. 4265–4273, 2008.

[11] G. Guan, T. Kida, T. Harada, M. Isayama, and A. Yoshida, "Photoreduction of carbon dioxide with water over $K_2Ti_6O_{13}$

photocatalyst combined with Cu/ZnO catalyst under concentrated sunlight," *Applied Catalysis A*, vol. 249, no. 1, pp. 11–18, 2003.

[12] H. J. Choi and M. Kang, "Hydrogen production from methanol/water decomposition in a liquid photosystem using the anatase structure of Cu loaded TiO_2," *International Journal of Hydrogen Energy*, vol. 32, no. 16, pp. 3841–3848, 2007.

[13] M.-S. Park and M. Kang, "The preparation of the anatase and rutile forms of Ag–TiO_2 and hydrogen production from methanol/water decomposition," *Materials Letters*, vol. 62, no. 2, pp. 183–187, 2008.

[14] B. S. Kwak, J. Chae, J. Kim, and M. Kang, "Enhanced hydrogen production from methanol/water photo-splitting in TiO_2 including Pd component," *Bulletin of the Korean Chemical Society*, vol. 30, no. 5, pp. 1047–1053, 2009.

[15] J.-J. Zou, H. He, L. Cui, and H.-Y. Du, "Highly efficient Pt/TiO_2 photocatalyst for hydrogen generation prepared by a cold plasma method," *International Journal of Hydrogen Energy*, vol. 32, no. 12, pp. 1762–1770, 2007.

[16] O. Rosseler, M. V. Shankar, M. K. L. Du, L. Schmidlin, N. Keller, and V. Keller, "Solar light photocatalytic hydrogen production from water over Pt and Au/TiO_2(anatase/rutile) photocatalysts: influence of noble metal and porogen promotion," *Journal of Catalysis*, vol. 269, no. 1, pp. 179–190, 2010.

[17] S. Xu and D. D. Sun, "Significant improvement of photocatalytic hydrogen generation rate over TiO_2 with deposited CuO," *International Journal of Hydrogen Energy*, vol. 34, no. 15, pp. 6096–6104, 2009.

[18] K. Lalitha, J. K. Reddy, M. V. Phanikrishna Sharma, V. D. Kumari, and M. Subrahmanyam, "Continuous hydrogen production activity over finely dispersed Ag_2O/TiO_2 catalysts from methanol: water mixtures under solar irradiation: a structure-activity correlation," *International Journal of Hydrogen Energy*, vol. 35, no. 9, pp. 3991–4001, 2010.

[19] T. Kawahara, T. Ozawa, M. Iwasaki, H. Tada, and S. Ito, "Photocatalytic activity of rutile-anatase coupled TiO_2 particles prepared by a dissolution-reprecipitation method," *Journal of Colloid and Interface Science*, vol. 267, no. 2, pp. 377–381, 2003.

[20] J. W. Park and M. Kang, "Synthesis and characterization of Ag_xO, and hydrogen production from methanol photodecomposition over the mixture of Ag_xO and TiO_2," *International Journal of Hydrogen Energy*, vol. 32, no. 18, pp. 4840–4846, 2007.

[21] V. Uvarov and I. Popov, "Metrological characterization of X-ray diffraction methods for determination of crystallite size in nano-scale materials," *Materials Characterization*, vol. 58, no. 10, pp. 883–891, 2007.

[22] C. Liu, X. Tang, C. Mo, and Z. Qiang, "Characterization and activity of visible-light-driven TiO_2 photocatalyst codoped with nitrogen and cerium," *Journal of Solid State Chemistry*, vol. 181, no. 4, pp. 913–919, 2008.

[23] B. Liu, X. Zhao, and L. Wen, "The structural and photoluminescence studies related to the surface of the TiO_2 sol prepared by wet chemical method," *Materials Science and Engineering B*, vol. 134, no. 1, pp. 27–31, 2006.

[24] J. F. Mouider, W. F. Stickle, P. E. Soboi, and K. D. Bomben, *Handbook of X-Ray Photoelectron Spectroscopy*, Perkin-Elmer Corporation, Eden Prairie, Minn, USA, 1992.